waveguide and the characteristics of a resonant waveguide section terminated by this admittance have been evaluated. Their correspondence with experimental data is found to be quite satisfactory. This allows one to set up a measurement technique which is nondestructive and needs only two measurements (VSWR and phase shift, or resonance frequency and Q factor). The relative permittivity can be calculated by means of computer-aided data processing and time-saving charts can be drawn for particular cases. The reflection coefficient approach allows a measurement of the material properties at all frequencies, limited only by the bandwidth of the waveguide. A good precision is obtained for the dielectric constant but the losses are determined only with an average 10-percent error due to the difficulty in measuring the phase shift. The cavity approach, on the other hand, overcomes this kind of inaccuracy but restricts the measurements to certain frequencies determined by the cavity geometry and the unknown material to be tested.

ACKNOWLEDGMENT

The authors wish to thank Prof. F. E. Gardiol for many helpful discussions and comments, V. Andriamiharisoa for his help with the computer programming, and O. Janz and M. Hermanjat for their precision mechanical work in preparing the material samples and the waveguide sensor. The numerical computations were performed on the CDC Cyber 7326 Computer of the EPF-L Computation Center.

REFERENCES

[1] H. M. Altschuler, "Dielectric constant," *Handbook of Microwave Measurements*, vol. 2, M. Sucher and J. Fox, Ed. New York: Polytechnic Press, 1963, pp. 495–548.
[2] F. E. Gardiol, "Nomograms save time in determining permittivity," *Microwaves*, vol. 12, pp. 68–70, Nov. 1973.
[3] M. C. Decréton and F. E. Gardiol, "Simple non-destructive method for the measurement of complex permittivity," *IEEE Trans. Instrum. Meas. (1974 Conf. Precision Electromagnetic Measurements)*, vol. IM-23, pp. 434–438, Dec. 1974.
[4] L. Lewin, *Advanced Theory of Waveguides*. London: Iliffe, 1951, ch. 6.
[5] R. T. Compton, "The admittance of aperture antennas radiating into lossy media," Antenna Lab., Research Foundation, Ohio State Univ., Columbus, Rep. 1691–5, Mar. 1964.
[6] J. Galejs, "Admittance of a waveguide radiating into stratified plasmas," *IEEE Trans. Antennas Propagat.*, vol. AP-13, pp. 64–70, Jan. 1965.
[7] M. C. Bailey and C. T. Swift, "Input admittance of a circular waveguide aperture covered by a dielectric slab," *IEEE Trans. Antennas Propagat.*, vol. AP-16, pp. 386–391, July 1968.
[8] C. T. Swift, "Admittance of a waveguide-fed aperture loaded with a dielectric plug," *IEEE Trans. Antennas Propagat.* (Commun.), vol. AP-17, pp. 356–359, May 1969.
[9] R. C. Rudduck and C. L. Yu, "Circular waveguide method for measuring reflection properties of absorber panels," *IEEE Trans. Antennas Propagat.*, vol. AP-22, pp. 251–256, Mar. 1974.
[10] M. C. Decréton, "Etude des phénomènes de diffraction électromagnétique au voisinage d'ouvertures, application à la mesure de petites distances et des propriétés des matériaux," Ph.D. dissertation, Ecole Polytechnique Fédérale, Lausanne, Switzerland, 1975.
[11] R. E. Collin, *Field Theory of Guided Waves*. New York: McGraw-Hill, 1960.
[12] N. Marcuvitz, *Waveguide Handbook*. Boston: M.I.T. Radiation Lab. Series no. 10, Tech. Pub., 1964, pp. 238–239.
[13] M. C. Decréton and V. Andriamiharisoa, "Non-destructive measurement of complex permittivity for dielectric slabs," in *Proc. 4th European Microwave Conf.* (Montreux, Switzerland, Sept. 1974), pp. 71–75.
[14] J. W. Bandler and P. A. McDonald, "Optimization of microwave networks by razor search," *IEEE Trans. Microwave Theory Tech. (Special Issue on Computer-Oriented Microwave Practices)*, vol. MTT-17, pp. 552–562, Aug. 1969.
[15] M. S. Ramachandraiah and M. C. Decréton, "A resonant cavity approach for the nondestructive determination of complex permittivity at microwave frequencies," *IEEE Trans. Instrum. Meas. (Special Issue on EEMTIC and IM Symp.)*, vol. IM-24, pp. 287–291, Dec. 1975.

Integrated Diode Phase-Shifter Elements for an X-Band Phased-Array Antenna

MARK E. DAVIS, MEMBER, IEEE

Abstract—**The design and production of 502 X-band P-I-N diode phase-shifter elements for a transmissive phased-array radar are presented. These elements consist of three phase-shifter states and two integrated dipole radiators formed using microwave integrated circuit techniques. The detailed design of loaded-line phase shifters and effects of circuit variations during production are examined in terms of measured performance. Finally, the performance of the phase shifters in the phased array is demonstrated through computed and measured antenna patterns giving quantitative results.**

INTRODUCTION

In a phased-array system where high-speed scanning, transmission reciprocity, and array weight are prime engineering concerns, P-I-N diode phase shifters are usually chosen. Considerable effort has been expended in the past ten years to arrive at the optimum design and lowest cost of P-I-N diode phase shifters for phased arrays. Several competitive factors dictate a design in each system that best meets the overall requirements of the phased-array radar. The factors that most contribute to the design of the phase shifter are the available space, coupling to the array radiator, location and complexity of the driver units, and finally, loss. Minimizing loss, while simultaneously optimizing the overall system design for both performance and cost effectiveness, usually becomes the most challenging engineering consideration.

The radiating element in a phased array has historically paced the phased-array performance. Because of the need to optimize the antenna directivity over a large scan volume, minimize mutual coupling effects on pattern gain, and maximize match with the transmitter/receiver circuitry, the radiator and the phase shifter have, in the past, been designed separately. This dictates a transition from the radiating element to the phase shifter and then to the feed distribution system. Due to this necessity of transitioning from one propagation medium to another, the overall design has increased loss due to mismatch reflections in the system. Typically, these transitions can add from 0.5 to 1.0 dB of loss to the element design at X band, depending on the frequency and transmission phase of the element. An even more important consideration than loss, however, is the increase in cost and reduction in reliability presented by having multiple connectors and transitions in the element design. An increased emphasis is placed on the "connectorless" element in phased-array design.

With these considerations, a novel approach to diode phase-shifter-element design was chosen in fabricating a large X-band transmissive phased-array antenna. The basic phase-shifter element is shown in Fig. 1. This design uses a loaded-line phase-shifter approach for the 45° and 90° sections. Loaded-line designs were chosen because of their compatibility with printed-circuit microstrip design and minimizing the number of diodes, and hence diode loss, required for the small phase-shift sizes. Two 45° sections are used in parallel to obtain the 90° desired phase shift. This was chosen in a trade-off of minimum diode loss, reflection loss, and fabrication ease over a hybrid-coupled or switched-line phase-shifter design [1]. For the 180° bit, a new design was chosen that gives an exact 180° of phase shift through coupling the microwave energy into the unbalanced propagation of a slot-guide transmission line etched in the microstrip ground plane [2]. This design will be presented in more detail in the next section of the paper.

Manuscript received April 28, 1975; revised September 2, 1975.
The author is with the Aircraft Equipment Division, General Electric Company, Utica, N. Y. 13503.

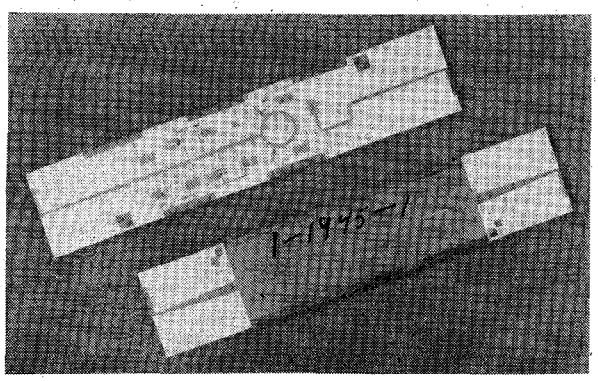

Fig. 1. Integrated P-I-N diode phase shifter and radiating dipoles.

The phased-array antenna is transmissive, using a dipole as the basic radiating element. For linear polarization, this dipole lends itself to simple and accurate integration with the microstrip phase shifter as seen in Fig. 1. The two poles are printed on opposite sides of the alumina substrate using the unbalanced mode of propagation of two-wire transmission line to match the dipole to the microstrip. This naturally establishes the two opposite senses of current density in the dipoles. Two such dipoles are printed on each element to provide the transmissive coupling of the electromagnetic energy in the lens array. When the element is placed in the array, the two metalized faces of the supporting structure serve as the ground planes for each dipole radiator.

From this brief overview of the phase-shifter-element selection, the following sections will develop the details of the design and production of an X-band phased-array element. A loaded-line phase shifter will be examined in terms of proper circuit design to minimize loss, maximize power handling capability, and, most importantly, ensure uniform phase and match characteristics in over 500 elements. On this basis, the results of over 500 elements will be examined and their performance in an 18-in-diam transmissive phased array will be presented.

PHASE-SHIFTER-ELEMENT DESIGN

The loaded-line phase shifter has been treated several times in the past [3]–[5]. Phase shift in the transmitted signal is obtained by changing the electrical phase of a section of line using the two reactive states of a semiconductor diode. Fig. 2 illustrates the equivalent-circuit concepts used in designing a loaded-line phase-shift bit. The transmission and reflection coefficients and their respective phases are calculated from the $ABCD$ transfer matrices

$$T = \frac{2}{A + B + C + D} \qquad \Gamma = \frac{A + B - C - D}{A + B + C + D}. \tag{1}$$

The circuit design was chosen so that the shunt susceptances are actually ac grounded through a quarter-wavelength open stub after the diode. This gives the transfer matrix

$$\begin{bmatrix} A & B \\ C & D \end{bmatrix} = \cos\theta_0 \begin{bmatrix} \left(1 - B_x \frac{a}{y_0}\right) & j\frac{a}{y_0} \\ j\left\{2B_x - \frac{(B_x^2 - y_0^2)a}{y_0}\right\} & \left(1 - B_x \frac{a}{y_0}\right) \end{bmatrix} \tag{2}$$

where $a = \tan\theta_0$. For proper match at the design center frequency, we require $B = C$

$$2B_x - (B_x^2 - y_0^2)\frac{a}{y_0} = \frac{a}{y_0}. \tag{3}$$

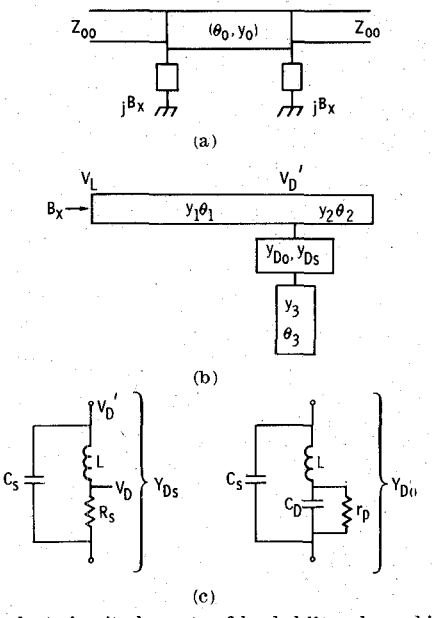

Fig. 2. Equivalent-circuit elements of loaded-line phase-shifter design. (a) Transmission-line π-section. (b) Shunt admittance equivalent circuit. (c) P-I-N diode equivalent circuit.

From the match condition (3), the required shunt susceptance for both desired phase shift and maximum energy transfer is given as the quadratic solution

$$B_x = \frac{y_0}{a} \pm K \tag{4}$$

where

$$K = [(1 + 1/a^2)y_0^2 - 1]^{1/2}. \tag{5}$$

Thus the transmission coefficient in the two states simplifies to

$$T = \left(\frac{a\cos\theta_0}{y_0}[\mp K + j]\right)^{-1} = |T|e^{j\psi}. \tag{6}$$

For a desired phase shift $\Delta\psi$, the required variation in the shunt susceptance is given by

$$K = \tan(\Delta\psi/2). \tag{7}$$

The circuit required to match the diode susceptance under forward and reverse bias depends on the characteristics of the diode chosen. For the X-band phase shifters discussed here, a special P-I-N diode was developed to minimize parasitic resistance and give the widest possible phase change between the two states. In this manner, the RF current through the diode, and hence the loss due to the series resistance of the diode, is minimized. This can be seen by considering the power dissipated in the diode P_D and the power incident on the line P_L [8]

$$\frac{P_D}{P_L} = \frac{I_D^2 R_s}{I_L^2 Z_{0o}} = \left(\frac{2\tan(\Delta\psi/2)}{V_D/V_L}\right)^2 \frac{R_s}{Z_{0o}}. \tag{8}$$

The voltage ratio V_D/V_L is determined by the ratio of the shunt-line admittance y_1 to the series-line admittance y_0. The characteristics of the X-band P-I-N diodes used are summarized as follows:

junction capacitance C_j	0.09 pF (at 10 V reverse);
gap stray capacitance C_s	0.02 pF;
load inductance L	0.55 nH;
series resistance R_s	1.2 Ω (10 mA forward);
parallel resistance	18 kΩ;
reverse breakdwon voltage	250 V minimum.

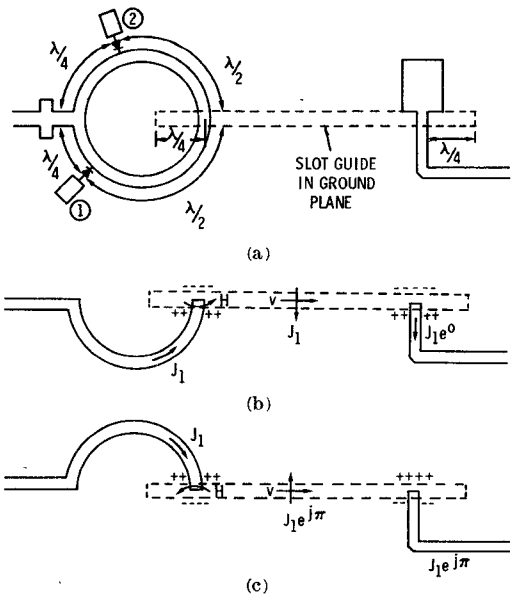

Fig. 3. Operation of slot-line coupled 180° phase-shifter design. (a) 180°-phase-shifter circuit. (b) Diode 2 short-circuited. (c) Diode 1 short-circuited.

With these parameters, the 45° design was chosen with $y_1 = 0.013$, $y_0 = 0.0208$. Thus the power dissipated per phase-shifter diode was only 0.03 dB.

The design of the 180° bit is more empirical [2]. It takes advantage of the odd-mode propagation in the slot-line transmission medium. Fig. 3 illustrates the operation of the device. A ring hybrid is designed with diode switches in an RF shunt configuration mounted a quarter-wavelength away from the microstrip junction and a half-wavelength from the slot-line junction etched in the microstrip ground plane. With diode 2 short-circuited and diode 1 reverse biased, all of the energy will transmit counterclockwise around the ring. Because of the position of the short a half-wavelength beyond the slot there is effectively an ac short to the ground plane at the slot position. With the microstrip oriented perpendicular to the slot, the concentric magnetic fields are oriented in the proper manner to establish a desired TE_{10} mode in the slot line. If this slot line is shorted a quarter-wavelength beyond the transition, the electromagnetic energy will propagate to the right with the phase velocity v of the slot guide. A transition back to the microstrip is located approximately one-half-wavelength to the right to allow transmission of energy through the phase shifter. In the opposite state of the two switches, the microwave energy travels clockwise around the ring and transitions into the slot with a π reversal of the current density. In this manner, an exact 180° of phase reversal is set up in the device. Further, because of the symmetrical nature of the ring hybrid, the frequency dependence of the phase shift will be zero to the first order.

To complete the element design, a dipole was constructed on each end. Transition to the dipole was accomplished using a two-wire transmission line described by Wheeler [7], [8]. The length of the dipole and the impedance of the two-wire line were determined experimentally in the array environment. This is necessary to obtain the optimum array-element pattern allowing for mutual coupling between elements. A single dipole with its microstrip transition was imbedded in an array of 60 identical dipoles, each of which was terminated in a matched load. By varying the dipole design and the dipole-to-ground plane spacing, the array element pattern shown in Fig. 4 was obtained.

PHASE-SHIFTER PRODUCTION RESULTS

Because the phase shifters described previously were designed to be used in a phased array, certain considerations had to be made in the fabrication. It is expected that both circuit fabrication tolerances

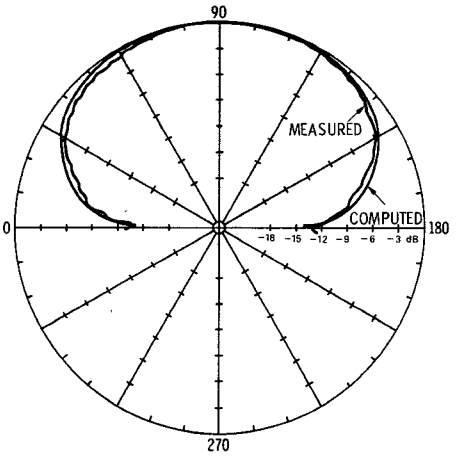

Fig. 4. Array element pattern of dipole compared to theoretical cosine directivity.

and diode characteristics will change from unit to unit. To individually construct each phase shifter would have the effect of considerably increasing the cost of the phased array. Nevertheless, excessive variances in the phase-shifter performance would have equally costly effects on the system due to increased signal loss and reduced bandwidth. Thus the circuits were etched, seven at a time, on one large-area (4-in by 4-in) substrate as shown in Fig. 5. Each phase shifter was then separated from the rest, using a digitally controlled YAG laser. This produced seven elements from a single unit that had mechanical tolerances of 0.001 in. Circuit-line etching tolerances were ±0.5 mil over the entire substrate; however, in any one sector, the standard deviation was less than 0.1 mil, as shown in Fig. 6.

Each phase shifter was tested using a computer-controlled microwave network analyzer. A test fixture with two X-band-waveguide-to-APC-7 adapters was made to give a low-VSWR transition from the waveguides to the two dipoles. With this analyzer, the transmission and reflection coefficients and phase of each of 502 elements in eight phase-shift states and 15 frequencies were measured.

The average phase shift and the rms deviation from this average

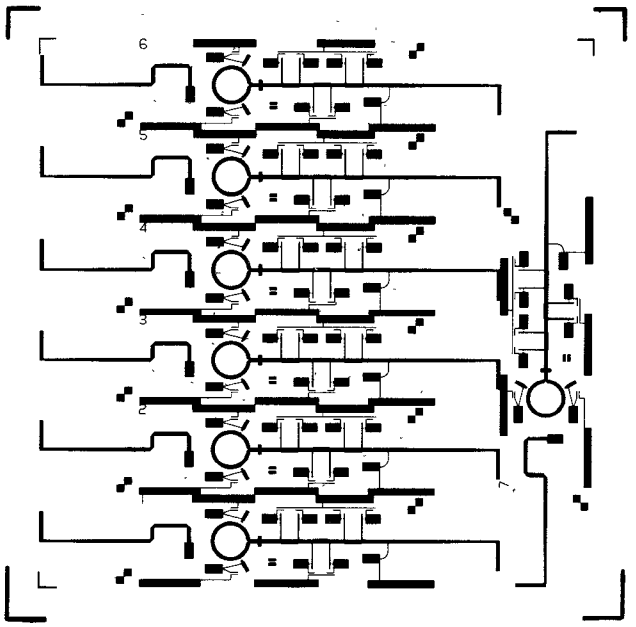

Fig. 5. Phase-shifter photomask for simultaneous fabrication of seven devices.

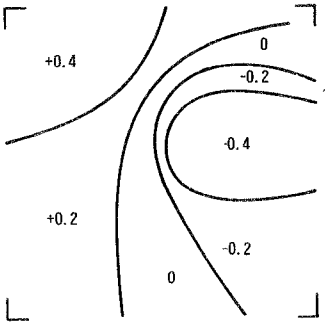

Fig. 6. Areas of median etch tolerances—deviation from desired linewidth.

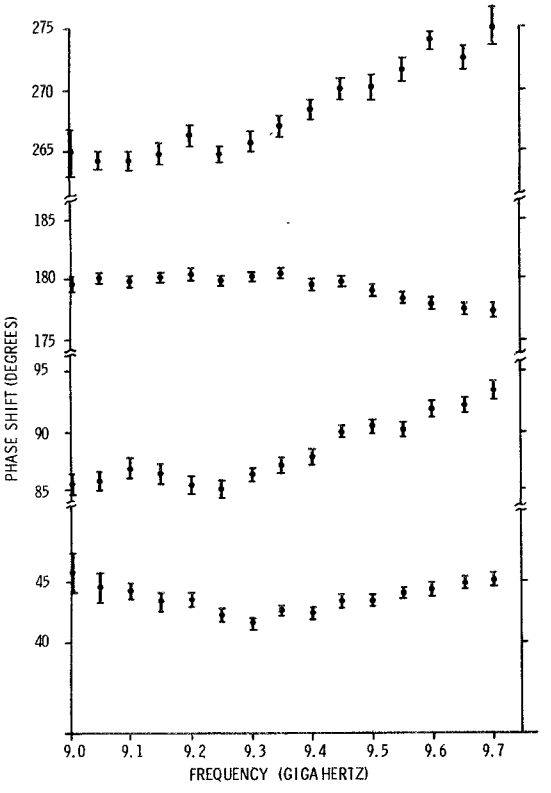

Fig. 7. Measured phase-shifter performance and standard deviation for 502-element production.

for all 502 phase shifters are shown in Fig. 7 for four of the eight states. A center frequency of 9.35 GHz was chosen with a desired bandwidth of ±5 percent. The data show that over this measured bandwidth the total phase shift in the three primary phase-shift states is accurate within 10 percent. The rms variation in the phase shift at any single frequency is generally less than 2 percent. Of particular importance is the 180° phase-shift design which is accurate to within 1 percent over the entire bandwidth with an rms variation of less than 1°.

The return loss of the phase shifter was measured and averaged −16 dB over the entire 700-MHz bandwidth with an rms deviation of 3 dB for all phase shifters within any 50-MHz bandwidth. The worst case VSWR was 2.1:1 near the band edge (9 7 MHz) This increase in VSWR partly explains the rise in apparent insertion loss of the elements at the band edges as shown in Fig. 8. A more important behavior of the elements, however, is the rms deviation of the insertion phase of all the elements. This insertion phase, the transmission phase of each element in its reference-phase state, determines the ability to focus the phased array and steer without

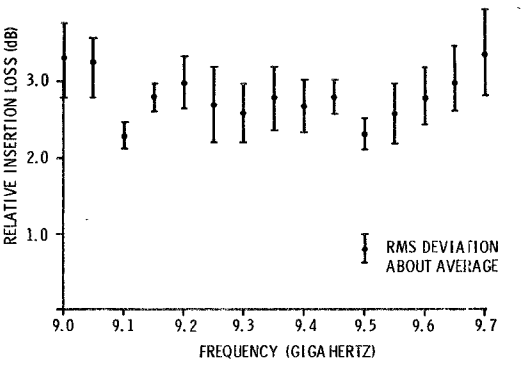

Fig. 8. Average insertion loss of 502 elements (reference phase state).

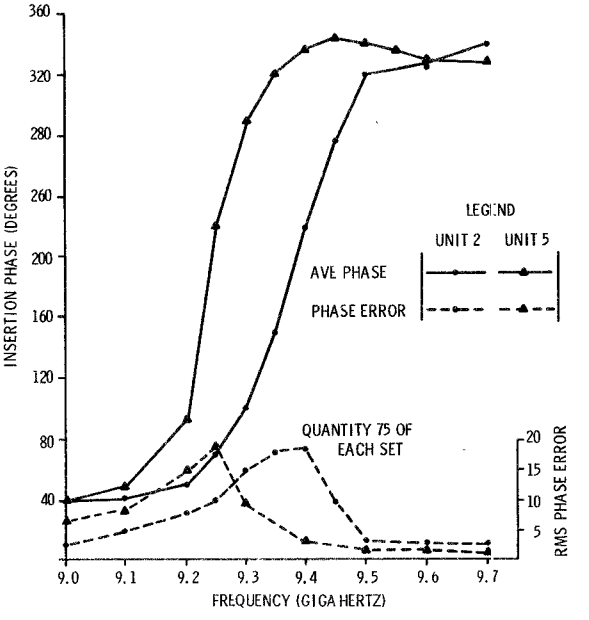

Fig. 9. Average insertion phase and root mean deviation about the average.

degradation of sidelobe levels. An rms phase error of 14°, for example, corresponds to a loss of approximately 1 dB of array gain. The average insertion phase and the rms deviation from this average are shown in Fig. 9 for two of the seven element types as numbered in Fig. 5. This separation of element types was necessary since the actual electrical length of each of the seven was compensated by 10 thousandths of an inch each, for a total spread of 60 mils from units 1 through 7.

As can be seen in Fig. 9, the insertion phase is very well-behaved except around the frequency where there is a large change of insertion phase with frequency. Generally an rms phase variation of less than 10° was experienced. However, at the center of the insertion phase, change as large as 19° rms was observed. It is not fully understood why the insertion phase does not vary linearly with frequency as would be expected for a loaded-line device. It is felt, however, that the phase change is greatest at the point that the 180° bit is most matched to the circuit. Because of the empirical nature of its design, it was observed to be critically dependent on the circuit match, phase, and amplitude, on both sides.

PHASED-ARRAY PERFORMANCE

The 502 phase shifters were assembled in a space-fed phased array as shown in Fig. 10. This array is illuminated with an X-band monopulse horn designed for a focal length of 12 in and for the radiation field to be −10 dB at the edge of the array. By this means

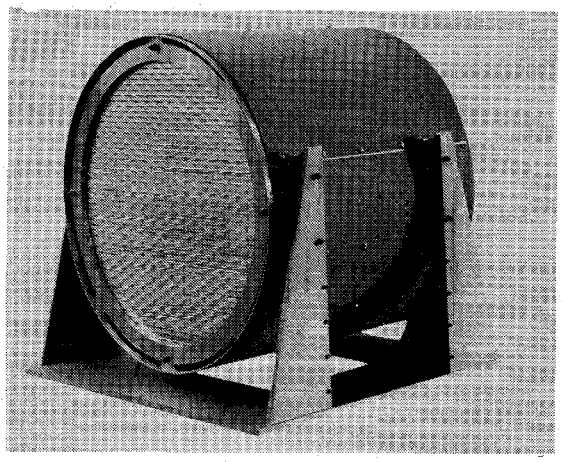

Fig. 10. Experimental X-band phased array.

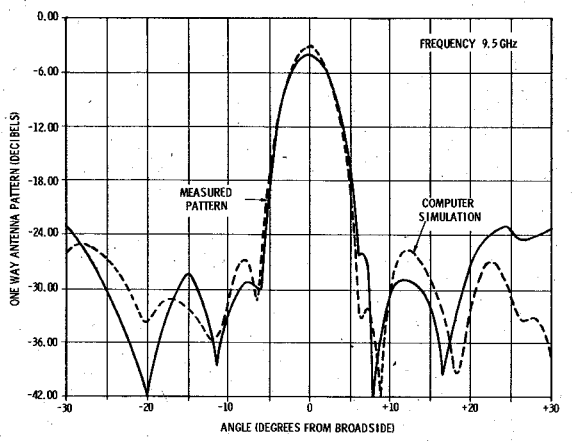

Fig. 11. Measured far-field performance of X-band phased array compared to simulated pattern.

an effective amplitude taper is obtained to reduce the peak sidelobes. Each phase shifter is driven by an integrated-circuit TTL logic-controlled driver located behind the lens area for cooling convenience. The signals are transmitted to each phase shifter by printed-wire Kapton flex cables.

Fig. 11 shows the measured array performance compared to the calculated far-field pattern. This far-field pattern was obtained using the actual measured phase shift, insertion phase, and loss assuming a cos θ array element pattern, and correcting for the space feed system. Excellent agreement exists in the pointing accuracy, beamwidth, and sidelobe levels. The array gain was measured within 1.5 dB of what had been calculated; however, this discrepancy has not been fully explained.

This performance illustrates the capability and necessity of fabricating phase shifters with fine phase and amplitude control. A design effort to minimize cost and weight produced a phased array weighing 50 lb, including structural housing and cooling manifold but excluding only power supplies and computer.

ACKNOWLEDGMENT

The author wishes to thank R. Hanrahan for taking the performance measurements of all the phase shifters. He would also like to acknowledge all the engineers at the General Electric Company who contributed to the design and fabrication of the ULTRA phased array. In particular, it should be recognized that D. Helms and P. P. Britt designed the phased-array element and Dr. J. McDade designed the diodes developed for the phase shifter.

REFERENCES

[1] J. F. White, "Diode phase shifters for array antennas," *IEEE Trans. Microwave Theory Tech. (Special Issue on Microwave Control Devices for Array Antenna Systems)*, vol. MTT-22, pp. 658–674, June 1974.

[2] P. P. Britt, "Antenna element including means for providing zero error 180° phase shift," U. S. Patent 3 803 621, Apr. 1974.

[3] J. F. White, "High power p-i-n diode controlled microwave transmission phase shifters," *IEEE Trans. Microwave Theory Tech.*, vol. MTT-13, pp. 233–242, Mar. 1965.

[4] C. W. Lee, "Diode phase shifter and coupler," G. E. Electronics Lab., Syracuse, N. Y., TIS R68ELS-6, Jan. 1968.

[5] F. L. Opp and W. F. Hoffman, "Design of digital loaded-line phase shift networks for microwave thin-film applications," *IEEE Trans. Electron Devices (Special Issue on Microwave Integrated Circuits)*, vol. ED-15, pp. 524–530, July 1968.

[6] M. E. Hines, "Fundamental limitations in RF switching and phase shifting using semiconductor diodes," *Proc. IEEE*, vol. 52, pp. 697–708, June 1964.

[7] H. A. Wheeler, "Transmission-line properties of parallel wide strips by a conformal-mapping approximation," *IEEE Trans. Microwave Theory Tech.*, vol. MTT-12, pp. 280–289, May 1964.

[8] ——, "Transmission-line properties of parallel strips separated by a dielectric sheet," *IEEE Trans. Microwave Theory Tech.*, vol. MTT-13, pp. 172–185, Mar 1965.